

**Preamble**

Although the coursework was initially presented as a C++ project, I took the liberty of rewriting the Ising Model system in a programming language called Google Go (<https://golang.org>). The motivation for this is Go has been designed to accommodate systems with high concurrency. This means that instead of simulating 1 system at a time, 10,000 different systems can be simulated simultaneously in different threads. This greatly increases time efficiency and has allowed me to achieve a significant level of statistical significance in my ensemble averages. Furthermore, this has also allowed me to use ergodicity to calculate time averages for a system ran over a long time period, for many different values of beta at the same time. To achieve the highest possible concurrent number of simulations, the results presented here were generated on a 32-core virtual private server. The source code for my implementation is accessible on Github: <http://tiny.cc/brb75y>.

# Comparison of Curie-Weiss Theory and Computation Metropolis Monte-Carlo Simulations for Modelling Phase Transitions in Ferromagnets using a Two-Dimensional Ising Model

**Candidate Number: 21594**

Department of Physics, University of Bath, Bath BA2 7AY, United Kingdom

**Abstract.** TODO

## 1. Introduction and Computational Method

Ferromagnetism is the property of a material to exhibit spontaneous magnetisation in the absence of an external magnetic field. The Ising Model is a mathematical model that uses the results of thermodynamics and statistical mechanics to describe how magnetic structure in some metals leads to ferromagnetism [2]. In the Ising Model presented in this paper, a magnetic material is modelled by a regular  $L \times L$  dimensional square lattice  $\Pi$ . A given grid point on this lattice  $\pi_{(i,j)} \in \Pi$  is indexed by cartesian coordinates  $(i, j)$  where  $i, j \in [0, L]$ . These coordinates are not strictly unique as periodic boundary conditions are applied so that a closed system is modelled. This is to say that the grid follows the mappings  $(i + \Lambda_i D, j + \Lambda_j D) \rightarrow (i, j)$  for  $\Lambda_i, \Lambda_j \in \mathbb{Z}$ . Each grid point  $\pi_{(i,j)}$  on this square lattice is assigned a discrete variable  $s_{(i,j)} \in \{0, 1\}$  that corresponds to the spin of the grid point. The system is therefore composed of  $N \equiv L^2$  spins. We arbitrarily define  $s_{(i,j)} = 1$  to represent 'spin up' and  $s_{(i,j)} = -1$  to represent 'spin down'. For a given grid point  $\pi_{(i,j)}$ , the convention of nearest neighbours is defined as representing the grid points directly adjacent to  $\pi_{(i,j)}$ , both vertically and horizontally, as shown in Figure 1. Using this convention, the energy of a given spin on the grid is defined as [2]

$$E_{(i,j)} = -h_{(i,j)} s_{(i,j)} \quad (1)$$

where

$$h_{(i,j)} = \sum_{(\alpha,\beta) \text{ n.n. of } (i,j)} [J s_{(\alpha,\beta)}] \quad (2)$$

Here "n.n" represents a sum over nearest neighbours and  $J$  is a positive real number with dimensions of energy that indicates the strength of the interactions between spins. Qualitatively, this set of equations defines the energy of a given spin as the sum of the interaction energies between the spin

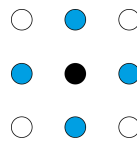


Figure 1: Each dot represents a grid point on the square lattice  $\Pi$ . The central black grid point represents the grid point  $\pi_{(i,j)}$ . The blue grid points represent the nearest neighbours of  $\pi_{(i,j)}$ . The white grid points represent points that are not considered nearest neighbours.

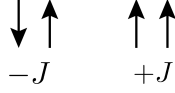


Figure 2: Two nearest neighbour spins on the grid have an interaction energy of  $-J$  if they are aligned and  $+J$  if they are not aligned.

and its nearest neighbours, where the interaction energy between two nearest neighbour spins is defined to be  $-J$  if the two spins are aligned and  $+J$  if the two spins are antiparallel [2], as shown in Figure 2.

From this definition of the energy for a single spin in the system, the total energy for the system is defined as

$$E = \frac{1}{2} \sum_{i,j} E_{(i,j)} \quad (3)$$

where the summation simply runs over every grid point in the square lattice. Furthermore, the magnetisation (per spin) of the system is defined as

$$\mathcal{M} = \frac{1}{N} \sum_{i,j} s_{(i,j)} \quad (4)$$

As the number of spins in the system is fixed, a canonical thermodynamic ensemble can be used to model the statistical behaviour of the system. If we let a microstate  $\mathcal{S}$  be defined by the instantaneous configuration of all the spins in the system, then the probability of finding the system in a microstate  $\mathcal{S}$  in thermal equilibrium with a heat bath at temperature  $T$  is given by statistical mechanics as [3] [2]

$$p_{eq}(\mathcal{S}) = \frac{1}{Z(T)} e^{-E(\mathcal{S})/k_B T} \quad (5)$$

where  $E(\mathcal{S})$  is the energy of microstate  $\mathcal{S}$  as given by equation (3) and  $k_B$  is the Boltzmann constant. The canonical partition function  $Z = Z(T)$  is used to enforce the normalisation condition  $\sum_{\mathcal{S}} p_{eq}(\mathcal{S}) = 1$  which gives the expression for  $Z$  as

$$Z(T) = \sum_{\mathcal{S}} e^{-E(\mathcal{S})/k_B T} \quad (6)$$

where the summations here run over all  $2^N$  possible microstates  $\mathcal{S}$  of the system.

In this paper, a Metropolis Monte Carlo method is used to investigate the properties  $E$  and  $\mathcal{M}$  of two dimensional Ising Model systems for different thermodynamic temperatures  $T$ . In the interest of being concise, for details on how the Metropolis Monte Carlo method works and is implemented, I refer the reader to standard literature [4]. In addition, we compare computational results with those given by a Curie-Weiss (mean-field) theory, the derivation and results of which are described in [2] and, in more detail, the chapter 'Phase Transitions and Critical Phenomena' of [1].

It is important to note that, in the computational simulations used in this paper, the Ising systems are characterised by a dimensionless temperature  $T_0 \equiv \frac{T k_B}{J}$ . From this, we define the inverse dimensionless temperature  $\beta \equiv \frac{1}{T_0}$ .

## 2. Method

### 2.1. Calculating Equilibrium Averages

Instead of calculating averages using an ensemble average as is conventional for statistical mechanical systems, it is in most cases also possible to calculate an average  $\langle \Gamma \rangle$  for a quantity of interest  $\Gamma$  by taking a time average, where time is proportional to the number of Monte Carlo sweeps completed in our case. This is the ergodic hypothesis of thermodynamics [3]. For the case of a simulated Ising

system, this means that average values can be determined by running a single simulation for a period of time as opposed to running many distinct simulations of that one system. In this way, an average value  $\langle \Gamma \rangle$  is determined by taking  $n$  samples  $\{\Gamma_i\}_{i=1}^n$  over a period of time. The average value is then calculated by [2]

$$\langle \Gamma \rangle = \frac{1}{n} \sum_{i=1}^n \Gamma_i \quad (7)$$

For independent measurements, the uncertainty in this average is estimated well by standard error.

When calculating equilibrium averages for properties of an Ising system, it is important to ensure the system has reached thermodynamic equilibrium before starting to take samples of the quantity being averaged. For all equilibrium averages presented in this paper, an integer  $n_0$  of Monte Carlo cycles are waited before sampling is begun. This is to give the system time to evolve through its initial transient behaviour as the system changes from the initial all spin down configuration to a state of equilibrium characterised by the thermodynamic temperature of the system. Furthermore, as the Metropolis Monte Carlo algorithm used in this paper is based on a Markovian random walk of phase space, subsequent samples of  $\Gamma$  are very likely to exhibit autocorrelation. Consequently, if a time average  $\langle \Gamma \rangle$  is to be representative of the system's entire equilibrium distribution for a practical number of samples  $n$ , it is necessary to only sample  $\Gamma$  every  $\Delta \in \mathbb{Z}^+$  Monte Carlo sweeps. This increases the likelihood that subsequent samples are independent. So, to account for both initial transient behaviour and to reduce the effect of autocorrelation, samples for equilibrium averages in this paper are taken at Monte Carlo times (sweep numbers)

$$t_i = n_0 + i\Delta \quad (8)$$

## 2.2. Calculating Derived Quantities

It can be shown that the specific heat capacity  $c$  and the magnetic susceptibility  $\chi$  of an Ising system are determinable by the equations [2]

$$c = \frac{1}{Nk_B T^2} \text{Var}(E) \quad (9) \quad \chi = \frac{N}{k_B T} \text{Var}(\mathcal{M}) \quad (10)$$

where  $T$  is the thermodynamic temperature of the Ising system and  $\text{Var}(E)$  and  $\text{Var}(\mathcal{M})$  refer to the variance of the system energy and magnetisation respectively.

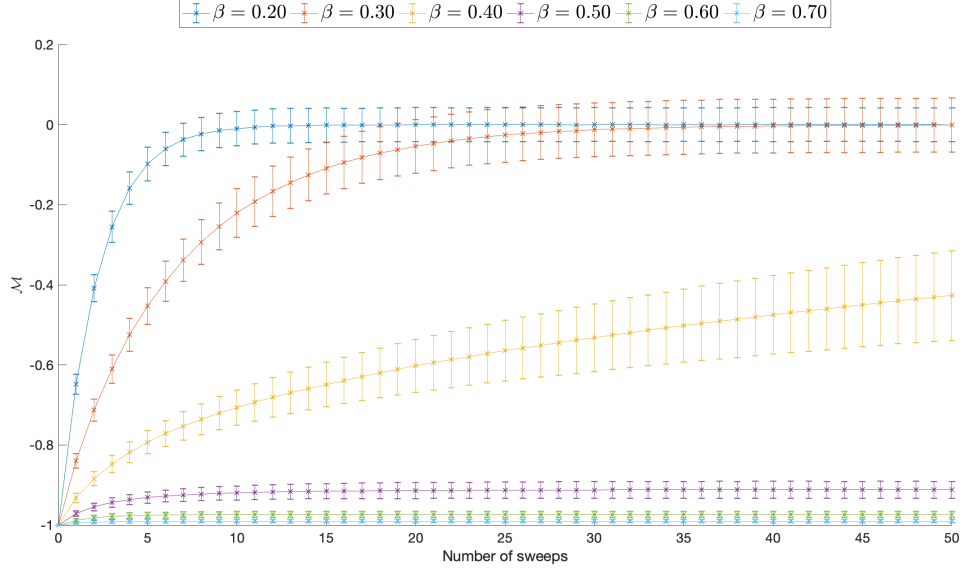
## 3. Results

### 3.1. Convergence to Equilibrium

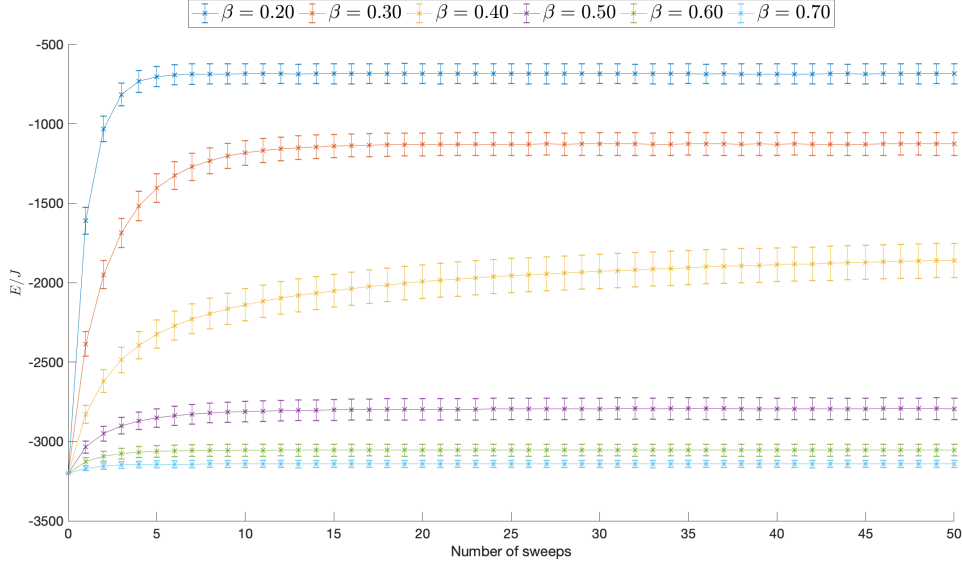
An Ising model simulation was prepared with all spins initially down. For different values of system temperature, as defined by the parameter  $\beta$ , the system was computationally simulated using the Metropolis Monte Carlo algorithm. The system's magnetisation per spin  $\mathcal{M}$  and dimensionless energy  $E/J$  were recorded as the number of Monte Carlo sweeps of the system was increased from 0 to 50. For each value of  $\beta$ , this simulation was run for an ensemble of 10,000 independent sub-systems, each with different pseudo-random number generator seeds. The evolution of system magnetisation as the number of Monte Carlo sweeps completed increases is shown in Figure 3 (a). Similarly, Figure 3 (b) shows the evolution of the system's dimensionless energy  $E/J$  as the number of Monte Carlo sweeps increases.

### 3.2. Measuring Equilibrium Averages

Figure 4 shows averages of quantities of interest as a function of dimensionless temperature  $T_0$  for an Ising system in thermal equilibrium. Figure 4 (a) shows the average magnetisation per spin as a function of  $T_0$ . Figure 4 (b) shows the average dimensionless energy per spin as a function of  $T_0$ .



(a) Evolution of system magnetisation per spin



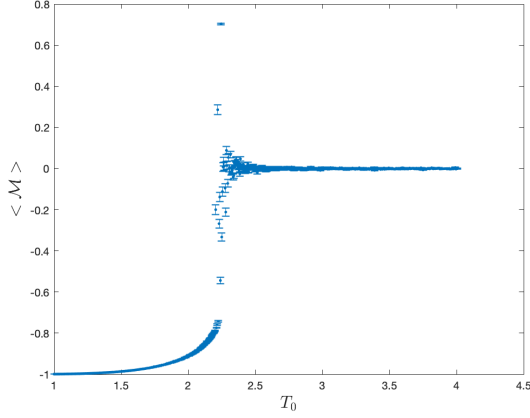
(b) Evolution of total system energy

Figure 3: Evolution of (a) system magnetisation per spin and (b) total system energy as a function of the number of Monte Carlo sweeps completed for a 2D Ising model simulation with all spins initially down. The simulation was ran for a set of systems with different thermodynamic temperatures, as defined by the parameter  $\beta$ . Each data point represents the ensemble average over  $n = 10,000$  independent sub-systems, each initialised with different pseudo-random number generator seeds. Error bars represent the standard deviation in the values of (a)  $\mathcal{M}$  and (b)  $\frac{E}{J}$  across the ensemble of systems.

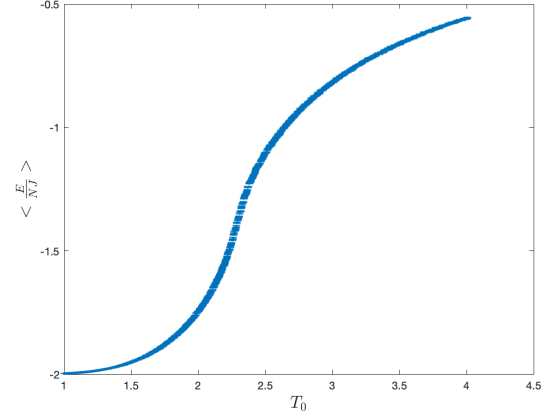
Figure 4 (c) shows the average of the absolute value of the magnetisation per spin as a function of  $T_0$ . For each of these graphs, the average value of interest is determined for dimensionless temperatures  $T_0 \in [1, 4]$  in discrete steps of  $\Delta T_0 = 0.005$ . Each average is calculated from 990 samples. The times that these samples were taken at is described by equation (8) with values  $n_0 = 2000$  and  $\Delta = 200$ .

### 3.3. Mean Field Theory

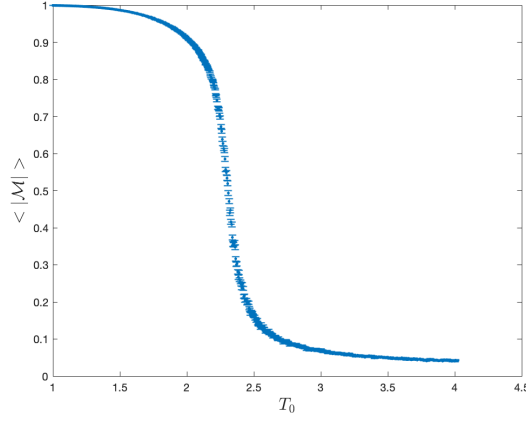
Figure 5 shows the mean field theory results for quantities of interest in the Ising model. Figure 5 (a) shows mean field theory results for the magnetisation per spin. Figure 5 (b) shows results for the



(a) Average magnetisation per spin



(b) Average dimensionless energy per spin



(c) Average absolute magnetisation per spin

Figure 4: Averages of quantities as given by equation (7) of interest as a function of dimensionless temperature  $T_0$  for an Ising system in thermal equilibrium. (a) shows average magnetisation per spin  $\langle \mathcal{M} \rangle$  vs  $T_0$ . (b) shows average dimensionless energy per spin  $\langle \frac{E}{NJ} \rangle$  vs  $T_0$ . (c) shows average absolute magnetisation per spin  $\langle |\mathcal{M}| \rangle$  vs  $T_0$ . Each average is determined from 990 samples given by equation (8) with  $n_0 = 2000$  and  $\Delta = 200$ . Error bars represent standard errors.

dimensionless energy per spin. Figure 5 (c) shows results for the dimensionless heat capacity. Figure 5 (d) shows results for the magnetic susceptibility.

### 3.4. Specific Heat Capacity and Magnetic Susceptibility

Figure 6 shows quantities derived from the data shown in Figure 4. Figure 6 (a) is a plot of a dimensionless quantity that is proportional to heat capacity as a function of dimensionless system temperature  $T_0$ . Figure 6 (b) is a plot of a dimensionless quantity that is proportional to magnetic susceptibility.

## 4. Discussion

### 4.1. Convergence to Equilibrium

For cases where the system evolves into a state with  $\mathcal{M} = 0$ , which is characterised by the system being in a state with approximately half the spins up and half the spins down, Figure 3 (a) shows that

an inverse temperature of  $\beta = 0.3$  takes longer to converge to this equilibrium state than  $\beta = 0.2$ .

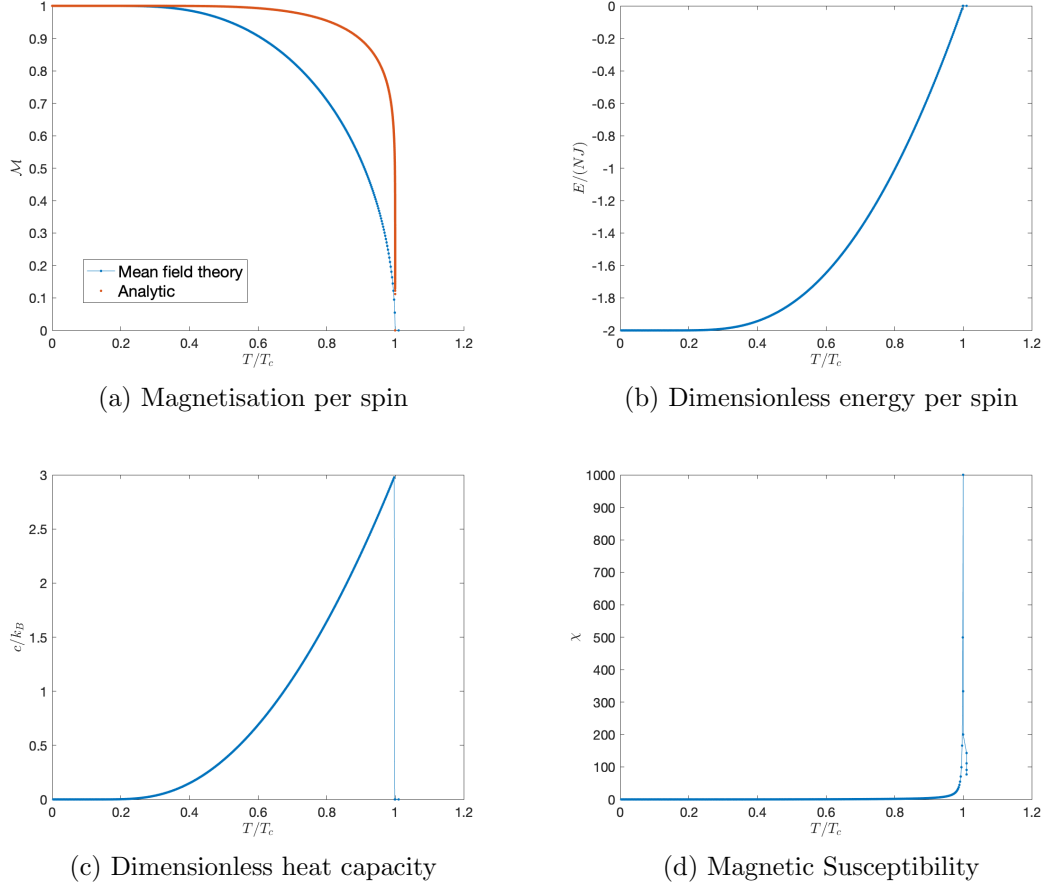


Figure 5: Mean field theory results for (a) the magnetisation per spin, (b) the dimensionless energy per spin, (c) dimensionless heat capacity and (d) magnetic susceptibility as a function of a dimensionless temperature parameter  $T/T_c$ . (a) also shows the analytic value of the magnetisation per spin as given in [2].

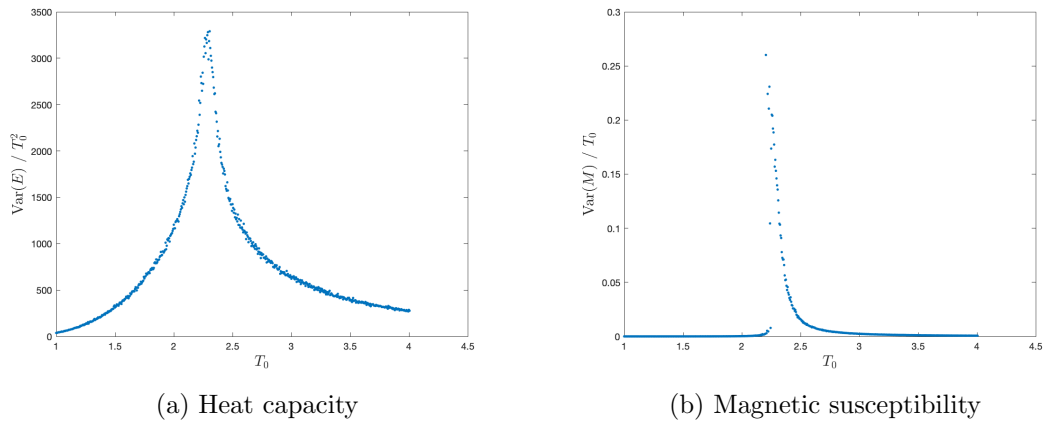


Figure 6: Computational results for dimensionless quantities that are proportional to (a) heat capacity and (b) magnetic susceptibility. Calculated from the data given in Figure 4.

#### 4.2. Equilibrium Averages

Figure 4 (a) shows an increase in system magnetisation from an initial value of  $-1$  to approximately  $-0.8$  as  $T_0$  is increased from 1 to approximately 2.3. This corresponds to the system transitioning from an initial perfectly ferromagnetic order with all spins down to more energetic states with ferrimagnetic order where some spins are up but the majority are still down, resulting in a net negative magnetisation. The simulated Ising model then almost-perfectly captures a phase transition at a critical dimensionless temperature of  $T_{0,c} \approx 2.3$ , at which point the system almost instantaneously assumes paramagnetic order for which  $\mathcal{M} = 0$  in the absence of an external magnetic field. For all temperatures greater than this critical temperature, no change in magnetisation is exhibited. Note somewhat weird behaviour is exhibited during the phase transition where the magnetisation appears to diverge and becomes greater than 0. This could be physical or could simply be that the system is so chaotic during this transition that Monte Carlo averaging breaks down and fails to capture the true behaviour of the system. Additionally, although a discontinuity exists in the magnetisation during the phase transition, the system's energy increases continuously during the transition, as physically expected!

#### 4.3. Comparison with Mean-Field Theory

#### 4.4. Derivative Quantities

#### 4.5. Suggestions for Improvement

When calculating averages in

### 5. Conclusion

### References

- [1] Modern Problems of Molecular Physics : Selected Reviews from the 7th International Conference “Physics of Liquid Matter: Modern Problems”, Kyiv, Ukraine, May 27–31, 2016. Springer Proceedings in Physics, 197. Springer International Publishing : Imprint: Springer, Cham, 2018.
- [2] RLJ AS, VJTR. Ising model coursework handout. ph30056 comp phys b – coursework 2: Ising model. Handout, 05 2019.
- [3] R. (Raymond) Jancel. Foundations of classical and quantum statistical mechanics. International series of monographs in natural philosophy ; Volume 19. Pergamon Press, Oxford, [England], first english edition. edition, 1969.
- [4] Tao Pang. An Introduction to Quantum Monte Carlo Methods. 2053-2571. Morgan and Claypool Publishers, 2016.